Converting Heat to Electrical Energy Using Highly Charged Polyoxometalate Electrolytes

Erik Svensson Grape,[a] Jiawei Huang,[ab] Dwaipayan Roychowdhury,[ab] Tekalign Debela,[a] Haeun Chang,[c] Andrew Jenkins,[a] Alina M. Schimpf,[cd] Christopher H. Hendon,[ab] Carl K. Brozek[ab]*

a. Department of Chemistry and Biochemistry, Material Science Institute, University of Oregon, Eugene, OR 97403, USA.

b. Oregon Center for Electrochemistry, University of Oregon, Eugene, Oregon 97403, United States.

c. Department of Chemistry and Biochemistry, University of California, San Diego, La Jolla, CA, United States

d. Program in Materials Science and Engineering, University of California, San Diego, La Jolla, CA, United States

**Corresponding author. Email: cbrozek@uoregon.edu*

Abstract: *Thermally regenerative electrochemical cycles and thermogalvanic cells harness redox entropy changes (ΔS_{rc}) to interconvert heat and electricity, with applications in heat harvesting and energy storage. Their efficiencies depend on ΔS_{rc} because it relates directly to the Seebeck coefficient, yet few approaches exist for controlling reaction entropy. Here, we demonstrate the use of highly charged molecular species in thermogalvanic devices. As a proof-of-concept, the highly charged Wells-Dawson ion $[P_2W_{18}O_{62}]^{6-}$ exhibits large ΔS_{rc} (-195 J mol^{-1} K^{-1}) and a Seebeck coefficient comparable to state-of-the-art electrolytes (1.1 mV K^{-1}), demonstrating the potential of linking the rich chemistry of polyoxometalates to thermogalvanic technologies.*

Greater than 60% of global energy exists as solar heat, geothermal heat, and waste heat from industrial sources with temperatures below 100 °C.[1,2] Recovering this so-called "low-grade heat" therefore offers a strategy for meeting society's energy demands while reducing its environmental impact. Solid-state thermoelectric devices convert heat to electrical energy by generating a voltage in response to a temperature gradient, with the magnitude of this response reported as the Seebeck coefficient (S_e). Despite decades of research, S_e for most solid-state thermoelectrics remains in the μV K^{-1} range,[3,4] prohibiting their use in harnessing low-grade heat. As an alternative, solution-state electrochemical cells may reach Seebeck coefficients in the mV K^{-1} range either as thermally regenerative electrochemical cycles (TRECs) or as thermogalvanic cells (TGCs).[5,6] Both technologies involve redox electrolytes that equilibrate to different mixtures of oxidized and reduced forms when exposed to different temperatures. This temperature dependence of the equilibrium constant produces a free energy difference (ΔG) between the electrodes at dissimilar conditions and hence a usable voltage. As exemplified in the relationship $\Delta G = \Delta H - T\Delta S$, the reversible redox entropy change (ΔS_{rc}) of the electrolyte dictates the magnitude of this temperature response. Equation 1 outlines how the S_e of a thermogalvanic device is proportional to ΔS_{rc}, where n is the number of electrons transferred in the redox reaction and F is Faraday's constant:

$$S_e = \frac{\Delta V}{\Delta T} = \frac{\Delta S_{rc}}{nF} \quad (1)$$

Optimizing the thermogalvanic effect therefore depends on tuning ΔS_{rc}, but few synthetic approaches exist for controlling the entropy of a reaction.

The Born expression for the electrostatic energetics of ion solvation provides a useful framework for

controlling ΔS_{rc}. Equation 2 shows an implication of this expression where ΔS_{rc} relates directly to the difference of squared charges (Z^2) of the oxidized and reduced species and inversely to the solvation radius (r). To test the applicability of this theoretical relationship, Weaver and Hupp evaluated the redox entropies of metal complexes in various solvents,[7] finding that ΔS_{rc} increases with increasing charge density of the redox pair as well as a smaller solvent Gutmann acceptor number.

$$\Delta S_{rc} \propto \frac{Z_{ox}^2 - Z_{red}^2}{r} \quad (2)$$

The high ΔS_{rc} of -135 J K^{-1} mol^{-1} observed for the $Fe(CN)_6^{4-/3-}$ couple,[8] the state-of-the-art thermogalvanic electrolyte, and its Seebeck coefficients of up to -1.6 mV K^{-1} can be ascribed to its high charge density, as predicted by Equation 2. Beyond charge state, this relationship also predicts that solvation radius dictates ΔS_{rc}. Indeed, the thermogalvanic activity of $Fe(CN)_6^{4-/3-}$ depends on parameters such as concentration of the redox-active species and the presence of additives that affect their solvation shell structure.[8–11] In addition to using redox couples with high charge densities, other synthetic strategies have been investigated for achieving higher S_e. Recent studies include the use of gel-based electrolytes,[12] deep eutectic solvents,[10] and ionic liquids,[13] and materials such as carbon nanotubes for creating thermogalvanic cells that display a high ionic conductivity while retaining a low thermal conductivity, in order to avoid thermal equilibration across the cell.[14] Additionally, the use of solvent mixtures,[8,15–18] polymers with redox-induced phase changes,[19] and supramolecular host-guest interactions[5,6,8] have shown promise for greatly altering the ΔS_{rc} for redox couples due to the concomitant ordering or release of solvent molecules following redox reactions. Although these recent studies employ varying methods for controlling solvation entropy, few have explored increasing charge density of the electrolyte.

In search of highly charged molecular redox pairs, polyoxometalates (POMs) serve as promising candidates due to their reversible redox chemistry, solubility, diverse compositions, and high charge states.[20–22] Since their discovery in the first half of the 19th century, POMs have been investigated for use in catalysis,[23] medicine,[24] and for applications related to their electronic and magnetic properties,[25,26] either as stand-alone molecules or as molecular materials.[27–30] Specifically, the α isomer of the Wells-Dawson (WD) polyoxotungstate anion, $[P_2W_{18}O_{62}]^{6-}$ (Figure 1a), has been shown to undergo a reversible six-electron reduction in four discrete steps, reaching a final charge state of -12.[31,32] Considering the high charge of the WD ion and its reversible redox chemistry in aqueous solutions, we evaluated its potential use in a thermogalvanic cell. First, to assess the impact of the unusually high charge state on the hydration shell of the WD anion, molecular dynamics (MD) simulations were carried out using the structure first published by Dawson as a starting point (see Supporting Information for details).[33] From the MD results, the solvent arrangement around WD^{6-}/WD^{7-} can be gauged by the number of hydrogen-bonded 1st, 2nd, and 3rd neighbors around each anion (Figure 1b), yielding 20 vs. 18, 47 vs. 45, and 76 vs. 102 contacts, for the -6 and -7 charge states, respectively. In this assessment, an upper donor-acceptor distance cutoff of 3.2 Å was used to probe the presence of strong-to-intermediate hydrogen bonds in the two

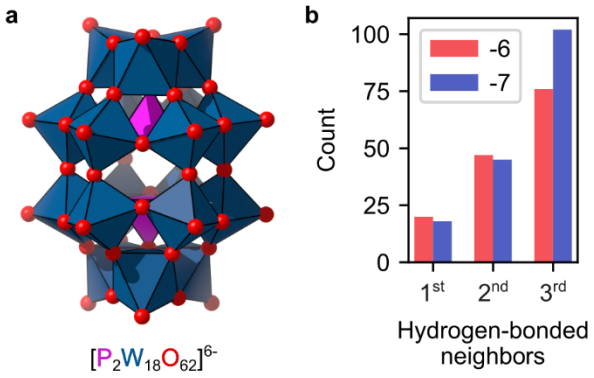

Figure 1. (a) Structure of the Wells-Dawson phosphotungstate ion, $[P_2W_{18}O_{62}]^{6-}$. (b) Bar plot showing the number of hydrogen-bonded 1st, 2nd and 3rd neighbors for water-solvated structures of the WD anion in the -6 and -7 charge state, as determined by molecular dynamics simulations (see Supporting Information for details).

structures.[34] These results indicate that the charge state of the WD influences the number of hydrogen bonds in the extended solvation shell, while the volume of the anionic cluster is barely affected by the reduction, with volumes of 1038 Å^3 and 1054 Å^3 for the -6 and -7 states, respectively, corresponding to an increase in volume of only 1.5 %. In other words, the change in charge state alters the solvation entropy without impacting solvation radius, rendering this system ideal for evaluating the Born expression in Equation 2.

To determine ΔS_{rc} for the WD anion, variable-temperature (VT) cyclic voltammograms (CVs) were acquired at a range of conditions in aqueous solutions (Supporting Information, Figure S2-S6). As described previously,[7] the temperature-dependent shift of a formal potential provides a direct measure of redox entropy. For details on the preparation of the potassium salt of the WD anion, $K_6[P_2W_{18}O_{62}]\cdot 14H_2O$, see Supporting Information. A typical CV scan can be seen in Figure 2a, showing four distinct reduction/oxidation steps, going from WD^{6-} to WD^{12-}, with the latter two redox features being two-electron processes.[31] For the VT-CV experiments, such as that shown in Figure 2b, a temperature range of approximately 5 to 50 °C was chosen and halfway potentials ($E_{1/2}$'s) were extracted for each of the four redox features in a variety of solvation conditions (see Supporting Information, Figure S2 – S8). As shown in Figure 2b, all redox features exhibit ΔS_{rc} comparable to $Fe(CN)_6^{4-/3-}$ of ca. 1 mV K^{-1} without optimization through solvent mixtures or other additives. For a preliminary study into altering hydration shell entropy, the effect of cation identity was studied through the collection of VT-CVs of WD solutions prepared in different acetate buffers (Li^+, Na^+, K^+, pH ≈ 5.1). Seebeck coefficients of -0.23, -0.44, and -0.49 mV K^{-1} for the first redox feature and -0.72, -0.75, -0.89 mV K^{-1} for the second redox feature were extracted for the Li-, Na- and K-acetate buffers, respectively. This apparent increase in temperature-dependence and the overall shift to less reducing halfway potentials (~20 mV for both redox features, Supporting Information, Figure S7) observed for the $Li^+/Na^+/K^+$ series could possibly be explained by the differences in cation size and the typical coordination number of each cation (Li^+ = 4, Na^+/K^+ = 6), altering the solvation of the WD cluster, effectively following the same trend as in the Hofmeister series.

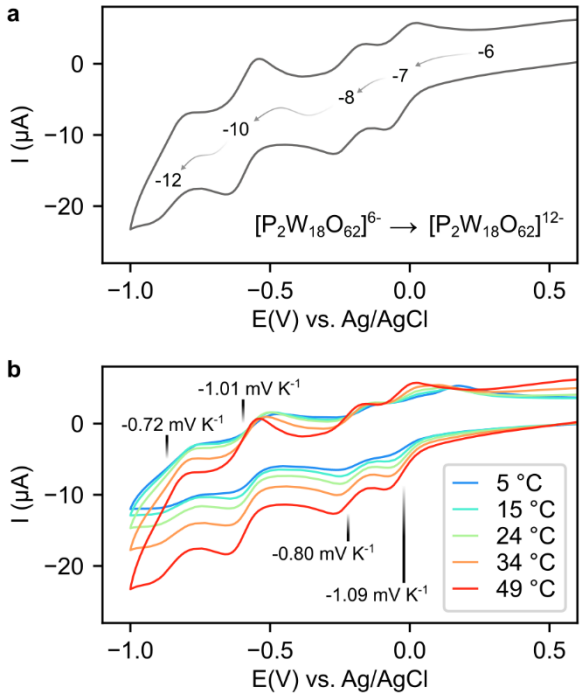

Figure 2. (a) A cyclic voltammogram of a 0.1 mM Wells-Dawson solution prepared in 0.1 M sodium acetate buffer (pH = 3.40, T = 49 °C). (b) Variable-temperature cyclic voltammograms of a 0.1 mM Wells-Dawson solution prepared in 0.1 M sodium acetate buffer (pH = 3.40) and the observed temperature-dependence of $E_{1/2}$ for the four redox features.

Across the range of studied aqueous conditions, S_e values for the different redox features range from approximately -0.23 to -1.66 mV K^{-1}, the largest being observed for the third redox feature in the K-acetate buffer solution. Seebeck coefficients of similar magnitude was also observed in WD solutions made from *N,N*-dimethylformamide and dimethyl sulfoxide (Supporting Information, Figure S9 and S10), yet focus was maintained on aqueous solutions out of practical considerations. For the VT-CV data in Figure 2b, the ΔS_{rc} of each redox process can be calculated following Equation 1, giving values ranging from -77 to -195 J mol^{-1} K^{-1}. Such redox entropy values are comparable and even higher than that of the well-studied ferro-/ferricyanide redox couple,

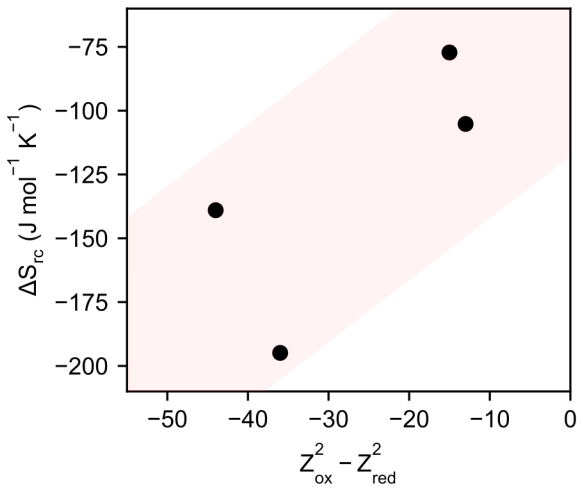

Figure 3. Plot showing redox entropy change as a function of the difference in charge states of redox pairs for a WD solution in 0.1 M sodium acetate buffer (pH = 3.40), showing an increase in redox entropy with higher charge states.

$Fe(CN)_6^{4-/3-}$ (ΔS_{rc} = 135 J mol^{-1} K^{-1}).[8] A plot of ΔS_{rc} as a function of the difference in charge states, similarly to what was presented by Hupp and Weaver for a range of metal complexes,[7] is shown in Figure 3. The trend of increasing ΔS_{rc} for redox pairs of higher charge, going from WD^{6-} to WD^{12-}, is possibly further amplified by the almost constant radius as indicated by MD simulations of the -6 and -7 charge states. Additionally, previous findings for another POM cluster, the Preyssler anion, $[P_5W_{30}O_{110}M^{n+}]^{(15-n)-}$ (M = encapsulated cation), have shown that the radius of gyration (R_g) of the anion remains constant independent of charge state, as studied using small-angle X-ray scattering (SAXS) and potential-controlled electrolysis, indicating that any structural changes following reduction/oxidation are too small to affect R_g.[35] As such, the observed relationship between ΔS_{rc} and charge state of the WD anion, as shown in Figure 3, as well as the MD results hint that the radius of the WD anion may, in a similar manner, remain more or less constant throughout the consecutive reduction/oxidation steps, while the hydration shell undergoes considerable restructuring to produce a large ΔS_{rc} predictable by the charge state of the cluster. Based on Equation 1 and assuming a constant radius for the WD redox pairs, an increase in S_e should be observed when going from the -6 state to states of a higher charge. Based on the VT-CV data, a general trend of increasing S_e for the for the highly charged redox couples can be observed, with Seebeck coefficients of e.g. -0.36 and -0.44 vs. -0.76 and -0.75 mV K^{-1} for the first two redox couples in sodium acetate solutions with a pH of 4.80 and 5.07, respectively (Supplementary Information, Table S1). This indicates that the highly charged redox couples generally yield not only higher ΔS_{rc}, but also larger Seebeck coefficients, owing to the more or less constant size of the anion.

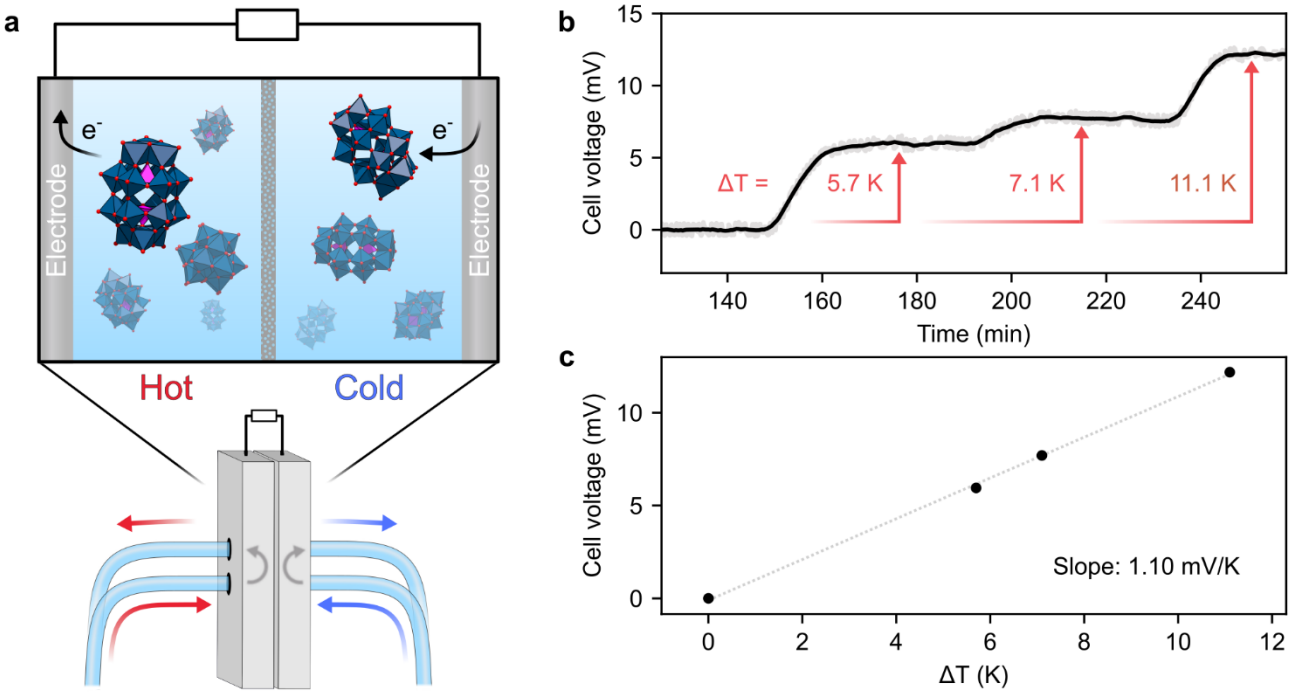

Figure 4. (a) Schematic of thermogalvanic flow cell where the hot and cold sides are separated by a Nafion membrane (for a detailed schematic, see Supporting Information). (b) Measured cell voltage of the thermogalvanic flow cell, showing a cell voltage of ~12 mV with a temperature difference of 11.1 K between the hot and cold solutions (1 mM WD solution made from 0.1 M sodium acetate buffer, pH = 5.5). (c) Observed cell voltage as a function of temperature difference (ΔT) for the thermogalvanic flow cell, showing a linear relationship.

To evaluate the possibility of converting heat into electrical energy using POMs, a thermogalvanic flow cell was constructed to determine the practical S_e of an aqueous WD solution (Figure 4a, see Supporting Information for additional details). For the flow-cell experiments, a 1 mM WD solution prepared from 0.1 M sodium acetate buffer (pH = 5.50) was used since WD solutions prepared with Na-acetate consistently showed well-resolved redox features across a large range of conditions. Following an equilibration period of 2.5 h at ambient conditions, the temperature difference across flow cell was raised to 5.7 K, 7.1 K and lastly 11.1 K in a step-wise manner over the course of ~2 h (Figure 4b). This process yielded a final cell voltage of 12.2 mV with a temperature difference of 11.K between the hot and cold side. The data in Figure 4b indicate a linear relationship between the temperature difference and the measured cell voltage, corresponding to a S_e of 1.10 mV K^{-1} (Figure 4c). As a control, a blank experiment was also carried out using a solution containing only Na-acetate, giving a Seebeck coefficient of 0.18 mV K^{-1} (Supplementary Information, Figure S11). It should be noted that WD anions of different redox states were not added to the solution, which has typically been used for thermogalvanic cell experiments using the ferri-/ferrocyanide redox couple.[9] Instead, allowing the system to equilibrate prior to applying a temperature gradient allows disproportionation to different redox states. These ease of cell preparation further highlights the potential utility of POM electrolytes in designing TRECs and TGCs.

In conclusion, this combined experimental-computational study demonstrates the applicability of the Born expression in identifying redox electrolytes for thermogalvanic devices competitive with state-of-the-art alternatives. Variable-temperature cyclic voltammetry measurements show reversible yet temperature-dependent behavior for aqueous WD solutions, exhibiting ΔS_{rc} in the range of -77 to -195 J mol^{-1} K^{-1} and Seebeck coefficients in the mV K^{-1} range at near-ambient temperatures using simple aqueous solutions of the WD anion. Additionally, a thermogalvanic cell was assembled using a sodium-acetate based WD solution, showing a Seebeck coefficient of 1.10 mV K^{-1}. The observed S_e could likely be further enhanced by altering any of the parameters readily accessible in this system of solutions alone (concentration, pH, cation species), as indicated by the range of responses seen when by altering the pH and varying the cation species. In addition to these modifications, the type of POM cluster could also be varied, as many POM species are highly soluble in a range of solvents and have been shown to undergo reversible reduction/oxidation. These include the well-known Keggin anion, $[PW_{12}O_{40}]^{3-}$, and the aforementioned Preyssler anion.[36,37] The richness of POM chemistry and the possibility of using lacunary or transition-metal functionalized POMs opens vast possibilities for altering thermogalvanic activity through tunable redox behavior and solvent interactions. From a general perspective, the high aqueous solubility observed for POM anions and the increasingly favorable solvation of POM anions with increasing charge, as well as their overall strong solvation,[38] render them particularly well suited for use in applications such as thermogalvanic cells. Taken together, these findings show that highly charged redox couples can be used to create thermogalvanic cells with Seebeck coefficients in the mV K^{-1} range by effectively maximizing the difference of Z_{ox}^2-Z_{red}^2, giving a high ΔS_{rc} and, in turn, a large S_e.

Supporting Information

The Supporting Information is available free of charge at http://pubs.acs.org.

All experimental details, spectroscopic data (IR, ^{31}P NMR), cyclic voltammetry data, and thermogalvanic flow cell data.

Acknowledgements

E. S. G. acknowledges support from the Swedish Research Council (grant no. 2022-06178). A.M.S. acknowledges support from the National Science Foundation through the Division of Materials Research under Grant DMR-2046269. C.H.H. acknowledges support from the National Science Foundation through the Division of Materials Research under Grant DMR-1956403C, the Research Corporation for Science Advancement (Cottrell Award), and the Camille and Henry Dreyfus Foundation. C. K. B. acknowledges support from the Department of Energy through the Office of Basic Energy Sciences under Grant DE-SC0022147 and the Research Corporation for Science Advancement (Cottrell Award).

References

(1) Van De Bor, D. M.; Infante Ferreira, C. A.; Kiss, A. A. Low Grade Waste Heat Recovery Using Heat Pumps and Power Cycles. *Energy* **2015**, *89*, 864–873. https://doi.org/10.1016/j.energy.2015.06.030.

(2) Papapetrou, M.; Kosmadakis, G.; Cipollina, A.; La Commare, U.; Micale, G. Industrial Waste Heat: Estimation of the Technically Available Resource in the EU per Industrial Sector, Temperature Level and Country. *Appl. Therm. Eng.* **2018**, *138*, 207–216. https://doi.org/10.1016/j.applthermaleng.2018.04.043.

(3) Hinterleitner, B.; Knapp, I.; Poneder, M.; Shi, Y.; Müller, H.; Eguchi, G.; Eisenmenger-Sittner, C.; Stöger-Pollach, M.; Kakefuda, Y.; Kawamoto, N.; Guo, Q.; Baba, T.; Mori, T.; Ullah, S.; Chen, X.-Q.; Bauer, E. Thermoelectric Performance of a Metastable Thin-Film Heusler Alloy. *Nature* **2019**, *576* (7785), 85–90. https://doi.org/10.1038/s41586-019-1751-9.

(4) He, J.; Tritt, T. M. Advances in Thermoelectric Materials Research: Looking Back and Moving Forward. *Science* **2017**, *357* (6358), eaak9997. https://doi.org/10.1126/science.aak9997.

(5) Zhou, H.; Yamada, T.; Kimizuka, N. Supramolecular Thermo-Electrochemical Cells: Enhanced Thermoelectric Performance by Host–Guest Complexation and Salt-Induced Crystallization. *J. Am. Chem. Soc.* **2016**, *138* (33), 10502–10507. https://doi.org/10.1021/jacs.6b04923.

(6) Xia, K. T.; Rajan, A.; Surendranath, Y.; Bergman, R. G.; Raymond, K. N.; Toste, F. D. Tunable Electrochemical Entropy through Solvent Ordering by a Supramolecular Host. *J. Am. Chem. Soc.* **2023**, *145* (46), 25463–25470. https://doi.org/10.1021/jacs.3c10145.

(7) Hupp, J. T.; Weaver, M. J. Solvent, Ligand, and Ionic Charge Effects on Reaction Entropies for Simple Transition-Metal Redox Couples. *Inorg. Chem.* **1984**, *23* (22), 3639–3644. https://doi.org/10.1021/ic00190a042.

(8) Inoue, H.; Zhou, H.; Ando, H.; Nakagawa, S.; Yamada, T. Exploring the Local Solvation Structure of Redox Molecules in a Mixed Solvent for Increasing the Seebeck Coefficient of Thermocells. *Chem. Sci.* **2024**, 10.1039.D3SC04955H. https://doi.org/10.1039/D3SC04955H.

(9) Buckingham, M. A.; Hammoud, S.; Li, H.; Beale, C. J.; Sengel, J. T.; Aldous, L. A Fundamental Study of the Thermoelectrochemistry of Ferricyanide/Ferrocyanide: Cation, Concentration, Ratio, and Heterogeneous and Homogeneous Electrocatalysis Effects in Thermogalvanic Cells. *Sustainable Energy Fuels* **2020**, *4* (7), 3388–3399. https://doi.org/10.1039/D0SE00440E.

(10) Antariksa, N. F.; Yamada, T.; Kimizuka, N. High Seebeck Coefficient in Middle-Temperature Thermocell with Deep Eutectic Solvent. *Sci. Rep.* **2021**, *11* (1), 11929. https://doi.org/10.1038/s41598-021-91419-5.

(11) Trosheva, M. A.; Buckingham, M. A.; Aldous, L. Direct Measurement of the Genuine Efficiency of Thermogalvanic Heat-to-Electricity Conversion in Thermocells. *Chem. Sci.* **2022**, *13* (17), 4984–4998. https://doi.org/10.1039/D1SC06340E.

(12) Wu, J.; Black, J. J.; Aldous, L. Thermoelectrochemistry Using Conventional and Novel Gelled Electrolytes in Heat-to-Current Thermocells. *Electrochim. Acta* **2017**, *225*, 482–492. https://doi.org/10.1016/j.electacta.2016.12.152.

(13) Abraham, T. J.; MacFarlane, D. R.; Baughman, R. H.; Jin, L.; Li, N.; Pringle, J. M. Towards Ionic Liquid-Based Thermoelectrochemical Cells for the Harvesting of Thermal Energy. *Electrochim. Acta* **2013**, *113*, 87–93. https://doi.org/10.1016/j.electacta.2013.08.087.

(14) Hu, R.; Cola, B. A.; Haram, N.; Barisci, J. N.; Lee, S.; Stoughton, S.; Wallace, G.; Too, C.; Thomas, M.; Gestos, A.; Cruz, M. E. D.; Ferraris, J. P.; Zakhidov, A. A.; Baughman, R. H. Harvesting Waste Thermal Energy Using a Carbon-Nanotube-Based Thermo-Electrochemical Cell. *Nano Lett.* **2010**, *10* (3), 838–846. https://doi.org/10.1021/nl903267n.

(15) Liu, Y.; Zhang, Q.; Odunmbaku, G. O.; He, Y.; Zheng, Y.; Chen, S.; Zhou, Y.; Li, J.; Li, M.; Sun, K. Solvent Effect on the Seebeck Coefficient of Fe2+/Fe3+ Hydrogel Thermogalvanic Cells. *J. Mater. Chem. A* **2022**, *10* (37), 19690–19698. https://doi.org/10.1039/D1TA10508F.

(16) Taheri, A.; MacFarlane, D. R.; Pozo-Gonzalo, C.; Pringle, J. M. The Effect of Solvent on the Seebeck Coefficient and Thermocell Performance of Cobalt Bipyridyl and Iron Ferri/Ferrocyanide Redox Couples. *Aust. J. Chem.* **2019**, *72* (9), 709–716. https://doi.org/10.1071/CH19245.

(17) Laws, K.; Buckingham, M. A.; Farleigh, M.; Ma, M.; Aldous, L. High Seebeck Coefficient Thermogalvanic Cells *via* the Solvent-Sensitive Charge Additivity of Cobalt 1,8-Diaminosarcophagine. *Chem. Commun.* **2023**, *59* (16), 2323–2326. https://doi.org/10.1039/D2CC05413B.

(18) Gao, C.; Liu, Y.; Chen, B.; Yun, J.; Feng, E.; Kim, Y.; Kim, M.; Choi, A.; Lee, H.; Lee, S. W. Efficient Low-Grade Heat Harvesting Enabled by Tuning the Hydration Entropy in an Electrochemical System. *Adv. Mater.* **2021**, *33* (13), 2004717. https://doi.org/10.1002/adma.202004717.

(19) Zhou, H.; Matoba, F.; Matsuno, R.; Wakayama, Y.; Yamada, T. Direct Conversion of Phase-Transition Entropy into Electrochemical Thermopower and the Peltier Effect. *Adv. Mater.* **2023**, *35* (36), 2303341. https://doi.org/10.1002/adma.202303341.

(20) Pope, M. T. Heteropoly and Isopoly Anions as Oxo Complexes and Their Reducibility to Mixed-Valence Blues. *Inorg. Chem.* **1972**, *11* (8), 1973–1974. https://doi.org/10.1021/ic50114a057.

(21) Gumerova, N. I.; Rompel, A. Synthesis, Structures and Applications of Electron-Rich Polyoxometalates. *Nat Rev Chem* **2018**, *2* (2), 0112. https://doi.org/10.1038/s41570-018-0112.

(22) Pope, M. T. Polyoxo Anions: Synthesis and Structure. In *Comprehensive Coordination Chemistry II*; Elsevier, 2003; pp 635–678. https://doi.org/10.1016/B0-08-043748-6/03035-8.

(23) Wang, S.-S.; Yang, G.-Y. Recent Advances in Polyoxometalate-Catalyzed Reactions. *Chem. Rev.* **2015**, *115* (11), 4893–4962. https://doi.org/10.1021/cr500390v.

(24) Rhule, J. T.; Hill, C. L.; Judd, D. A.; Schinazi, R. F. Polyoxometalates in Medicine. *Chem. Rev.* **1998**, *98* (1), 327–358. https://doi.org/10.1021/cr960396q.

(25) Lehmann, J.; Gaita-Ariño, A.; Coronado, E.; Loss, D. Spin Qubits with Electrically Gated Polyoxometalate Molecules. *Nat. Nanotechnol.* **2007**, *2* (5), 312–317. https://doi.org/10.1038/nnano.2007.110.

(26) Clemente-Juan, J. M.; Coronado, E.; Gaita-Ariño, A. Magnetic Polyoxometalates: From Molecular Magnetism to Molecular Spintronics and Quantum Computing. *Chem. Soc. Rev.* **2012**, *41* (22), 7464. https://doi.org/10.1039/c2cs35205b.

(27) Coronado, E.; Gómez-García, C. J. Polyoxometalate-Based Molecular Materials. *Chem. Rev.* **1998**, *98* (1), 273–296. https://doi.org/10.1021/cr970471c.

(28) Long, D.-L.; Burkholder, E.; Cronin, L. Polyoxometalate Clusters, Nanostructures and Materials: From Self Assembly to Designer Materials and Devices. *Chem. Soc. Rev.* **2007**, *36* (1), 105–121. https://doi.org/10.1039/B502666K.

(29) Miras, H. N.; Vilà-Nadal, L.; Cronin, L. Polyoxometalate Based Open-Frameworks (POM-OFs). *Chem. Soc. Rev.* **2014**, *43* (16), 5679–5699. https://doi.org/10.1039/C4CS00097H.

(30) Chen, L.; Turo, M. J.; Gembicky, M.; Reinicke, R. A.; Schimpf, A. M. Cation-Controlled Assembly of Polyoxotungstate-Based Coordination Networks. *Angew. Chem. Int. Ed.* **2020**, *59* (38), 16609–16615. https://doi.org/10.1002/anie.202005627.

(31) Pope, M. T.; Papaconstantinou, E. Heteropoly Blues. II. Reduction of 2:18-Tungstates. *Inorg. Chem.* **1967**, *6* (6), 1147–1152. https://doi.org/10.1021/ic50052a018.

(32) Chen, J.-J.; Symes, M. D.; Cronin, L. Highly Reduced and Protonated Aqueous Solutions of [P2W18O62]6− for on-Demand Hydrogen Generation and Energy Storage. *Nat. Chem.* **2018**, *10* (10), 1042–1047. https://doi.org/10.1038/s41557-018-0109-5.

(33) Dawson, B. The Structure of the 9(18)-Heteropoly Anion in Potassium 9(18)-Tungstophosphate, $K_6(P_2W_{18}O_{62}).14H_2O$. *Acta Crystallogr.* **1953**, *6* (2), 113–126. https://doi.org/10.1107/S0365110X53000466.

(34) Steiner, T. The Hydrogen Bond in the Solid State. *Angew. Chem. Int. Ed.* **2002**, *41* (1), 48–76.

(35) Antonio, M. R.; Chiang, M.-H.; Seifert, S.; Tiede, D. M.; Thiyagarajan, P. In Situ Measurement of the Preyssler Polyoxometalate Morphology upon Electrochemical Reduction: A Redox System with Born Electrostatic Ion Solvation Behavior. *J. Electroanal. Chem.* **2009**, *626* (1–2), 103–110. https://doi.org/10.1016/j.jelechem.2008.11.009.

(36) Pope, M. T.; Varga, G. M. Heteropoly Blues. I. Reduction Stoichiometries and Reduction Potentials of Some 12-Tungstates. *Inorg. Chem.* **1966**, *5* (7), 1249–1254. https://doi.org/10.1021/ic50041a038.

(37) Antonio, M. R.; Williams, C. W.; Soderholm, L. Synthesis and Characterization of Actinide-Exchanged Preyssler Heteropolyanions [AnP5W30O110]N− (An≡Th, Am, Cm). *J. Alloys Compd.* **1998**, *271–273*, 846–849. https://doi.org/10.1016/S0925-8388(98)00231-X.

(38) Dullinger, P.; Horinek, D. Solvation of Nanoions in Aqueous Solutions. *J. Am. Chem. Soc.* **2023**, jacs.3c09494. https://doi.org/10.1021/jacs.3c09494.